A Spectrally-Accurate FVTD Technique for Complicated Amplification and Reconfigurable Filtering EMC Devices

Nikolaos V. Kantartzis[1], Stylianos D. Assimonis[1], Antonios X. Lalas[1],
Jonathan B. Scott[2], and Christos S. Antonopoulos[1]
[1]Dept. of Electrical and Computer Engineering, Aristotle University of Thessaloniki, GR-54124 Thessaloniki, Greece
[2]School of Engineering, The University of Waikato, Hamilton 3240, New Zealand
E-mail: chanto@auth.gr

Abstract — The consistent and cost-effective analysis of complex amplification and filtering structures, is introduced in this paper by means of a novel spectrally-precise FVTD method. The proposed scheme combines enhanced spatial derivative approximators in general curvilinear coordinates with a fully conservative field flux formulation. Hence, a class of 3-D operators which assign the proper weights to each spatial increment is developed. For periodic EMC components, the computational space is separated to a number of dual subdomains. Numerical results from different realistic setups validate our method and prove its applicability.

I. INTRODUCTION

The evolution of accurate time-domain algorithms for complex electromagnetic compatibility (EMC) structures remains an issue of an ongoing research. Among various applications, amplification and reconfigurable filters are proven really critical in the design of modern electromagnetic systems [1]-[4]. Bearing in mind that many of these devices should be redesigned to correspond to the repeatedly rising standards, it is obvious that the use of consistent models can be an effective tool to reduce high fabrication costs. Such a process, however, is often rather laborious, as most of the systems have fine details that need large resources. To this aim, diverse techniques – pursuing inherent-error improvements – have been so far derived [5]-[7], while, from an application point of view, a method which gives an exact solution for the triode problem has been given in [8].

In this paper, a 3-D finite-volume time-domain (FVTD) method with an enhanced spectral resolution is presented for the rigorous analysis of demanding EMC components. Two typical categories are the amplification devices, like improved triodes, and microstrip-oriented filters that incorporate electromagnetic bandgaps (EBGs) in a periodic uniform or non-uniform fashion. The new scheme introduces derivative approximators of controllable order based on a conservation-law concept, which expresses all terms as components of a solution vector. Regarding periodicity, the algorithm divides the space in subdomains and associates their field quantities to dual topologies in the sense of differential forms. Experimental data from fabricated prototypes are compared to several numerical simulations, revealing the ability of our formulation to accurately predict the device's overall performance, before the process of manufacturing.

II. THE SPECTRALLY-CONTROLLABLE FVTD ALGORITHM

The proposed method develops a curvilinear dual-cell grid with higher-order derivative approximations of adjustable spectral accuracy. It, also, launches a stable integration scheme that conserves the total charge in a global sense. So, the staggered-meshed finite-difference time-domain (FDTD) formalism is efficiently overcome with a reasonably limited overhead.

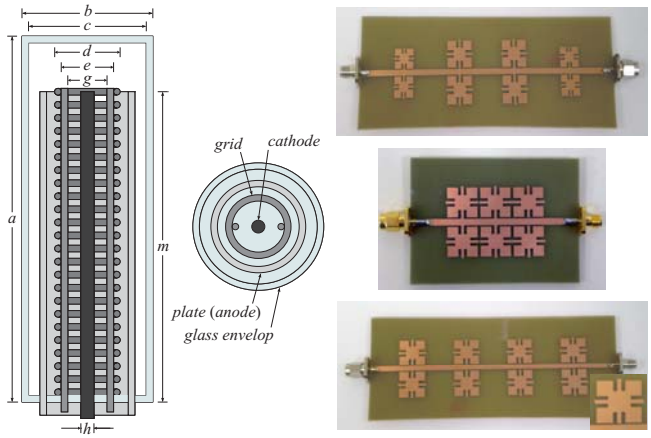

Fig. 1. (a) Geometry of an improved triode. (b) Fabricated prototypes of three uniform/non-uniform cross/gap EBG-loaded reconfigurable filters.

Since the novel FVTD technique utilizes arbitrary cells, with the four corners of their faces not necessarily lying on the same plane, it is essential to describe the geometry of all edges and faces in both lattices. Hence, unit vector direction cosines are introduced to transform Maxwell's equations in the form of

$$\varepsilon\frac{\partial \mathbf{E}}{\partial t}-\boldsymbol{\mathcal{W}}(\mathbf{H})+\sigma\mathbf{E}=-\mathbf{J}_s \quad \text{and} \quad \mu\frac{\partial \mathbf{H}}{\partial t}+\boldsymbol{\mathcal{W}}(\mathbf{E})=\mathbf{0}\,, \tag{1}$$

$$\boldsymbol{\mathcal{W}}(\mathbf{F})=\begin{bmatrix} S_v^L F_w - S_w^L F_v \\ S_w^L F_u - S_u^L F_w \\ S_u^L F_v - S_v^L F_u \end{bmatrix}+\sum_{i=1}^{L}\left(q_1 S_u^L + q_2 S_v^L + q_3 S_v^L\right)\mathbf{F}\,, \tag{2}$$

with (u,v,w) being a general coordinate system, vector $\mathbf{F}$ standing for the electric, $\mathbf{E}$, or magnetic, $\mathbf{H}$, field vector and L denoting the accuracy order in the computation of spatial derivatives. Specifically, the total spectral-resolution performance can be effectively controlled through the enhanced operator

$$S_\eta^L\left[F\big|_{u,v,w}^t\right]=\frac{e^{L\Delta\eta/6}}{2\sqrt{\pi}\Delta\eta}M_{\eta,P}^L\left[F\big|_{u,v,w}^t\right]+\sum_{\kappa=1}^{3}\left(1+\frac{\Delta\eta}{4\kappa}\right)F\big|_{\eta\pm\kappa\Delta\eta}^t\,, \tag{3}$$

where $\eta\in(u,v,w)$ and $\Delta\eta\in(\Delta u,\Delta v,\Delta w)$ is the spatial increment. Moreover, spatial form $M_{\eta,D}[.]$ enables the fine adjustment of spectral accuracy via diverse stencils and weighting coefficient P. In particular, considering the $g(u,v,w)$ system metrics,

$$M_{\eta,P}^L\left[F\big|_{u,v,w}^t\right]=g(u,v,w)\sum_{l=1}^{L}\Lambda_l^\eta\left\{\sum_{p=1}^{P}N_{l,p}^\eta\,F\big|_{u,v,w}^t\right\}\,. \tag{4}$$

Structural parameters Λ_l and $N_{l,p}$ increase the consistency of the algorithm during the modeling of complex geometric details or material discontinuities, like the realistic EMC devices of Fig. 1. In fact, such a concept leads to node sets which provide rapid interface extrapolations with all possible topologies.

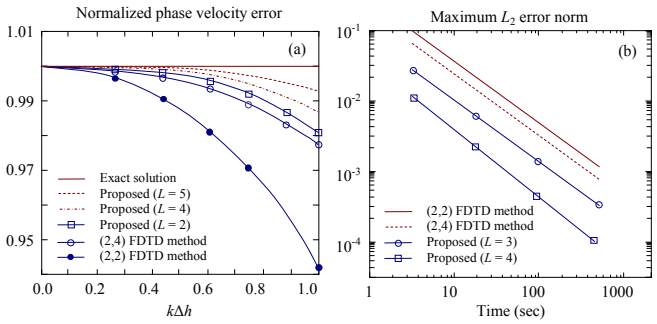

Fig. 2. (a) Normalized phase velocity error and (b) maximum L_2 error norm for the proposed and various higher-order time-domain realizations.

Apart from the Lth-order spatial operator in (2), which increases the spectral order of accuracy, parameters q_1, q_2, q_3 guarantee the stability of the resulting schemes and subdue potential late-time oscillations. To exploit all fluxes through the element faces, we introduce the cell average notion – i.e. the average of vector $\mathbf{F} = [\mathbf{E}, \mathbf{H}]^T$ at the barycenter of the cell – as

$$F_i = \frac{1}{V_i}\iiint_{V_i} \mathbf{F}(\mathbf{r})dV \ , \qquad (5)$$

with $\mathbf{r}$ the position vector and V_i the volume of cell i. In this context, two subvectors of $\mathbf{F}$ are considered; one on the internal and the other on the external side of each face. Both quantities are computed by an interpolation approach centered on the respective face side. Setting these issues to (1), (2), one gets

$$\partial_t \mathbf{F} + \mathbf{Z}\mathbf{F} = \mathbf{\Xi} \ , \qquad (6)$$

for $\mathbf{Z}$ a matrix with all material properties and $\mathbf{\Xi}$ a term containing the source contributions of every grid cell. To complete our FVTD method, time derivatives in (1) are precisely approximated via the leapfrog-like, predictor-corrector scheme of

$$\mathbf{F}^{n+1/2} = \mathbf{F}^{n} - 0.5\Delta t\mathbf{A}\mathbf{F}^{n} \quad \text{and} \quad \mathbf{F}^{n+1} = \mathbf{F}^{n} - 0.5\Delta t\mathbf{A}\mathbf{F}^{n+1/2} \ , \ (7)$$

in which $\mathbf{A}$ is the usual update matrix for vector $\mathbf{F}$. It is stated that the proposed algorithm is conditionally stable, obeying to a less strict (than the FDTD) Courant-type criterion, extracted through the von Neumann analysis. The above assets along with the parametrized adjustment of the spectral resolution, improve significantly the dispersion relation (as clearly shown in Fig. 2), which, compared to the typical $\mathcal{G}_{\text{FDTD}}$ one, reads

$$\sin^2\left(\frac{\omega\Delta t}{2}\right) = \frac{21(\Delta t)^{3/5}}{8(\mu\varepsilon)^{1/2}}\mathcal{G}_{\text{FDTD}} \ , \qquad (8)$$

with Δt representing the algorithm's temporal increment.

III. NUMERICAL RESULTS – CONCLUSIONS

The first application for the certification of the proposed FVTD method is the improved triode of Fig. 1a. Its dimensions are: a = 5.6 cm, b = 2 cm, c = 1.8 cm, d = 1 cm, e = 0.8 cm, g = 0.6 cm, h = 0.2 cm, and m = 4.75 cm, whereas for the termination of the domain, a 6-cell thick PML is employed. Apparently, the discretization of this geometry is very demanding, especially due to its large electrical size and curved parts. For our simulations, an L = 3, 4 or 5 order of spectral accuracy is deemed adequate, thus leading to the very coarse 42×26×40 lattice. Figure 3 illustrates the triode plate versus plate potential for different grid voltages of the triode. As observed, our technique is proven very accurate compared to the results acquired by the finite element method, which, however, requires a 65% finer mesh.

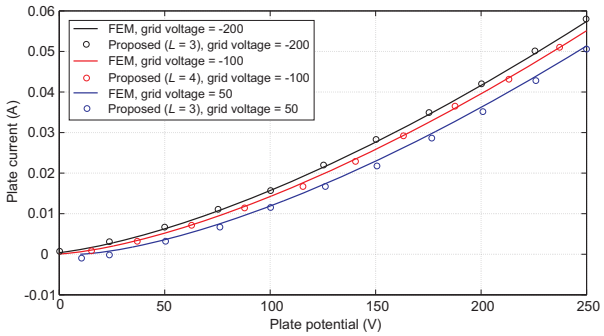

Fig. 3. Simulated triode plate current curves versus plate potential.

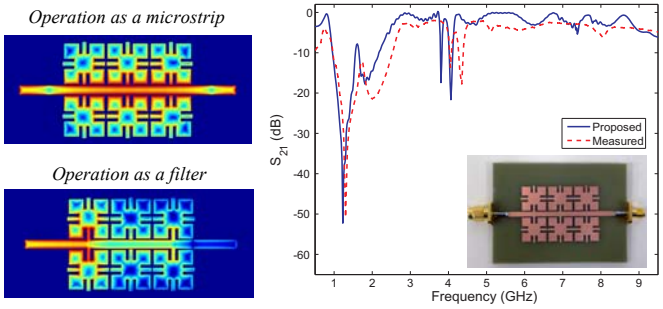

Fig.4. Snapshots of the surface current distribution and S_{21} simulated and measured results for a uniform cross/gap EBG-loaded microwave filter.

Next, let us proceed to the reconfigurable filtering structures of Fig. 1b. The basic element of these devices is a 2.8 mm-wide microstrip line loaded with two cross or 'gap' EBG unitcells. The height of the unicell is 15.24 mm, the size of the gap is 0.4 mm, and the thickness of the ε_r = 4.5 substrate is 1.5mm. As shown in Fig. 1b, both uniform and unevenly distributed unitcell configurations are investigated. To this end, the input port is excited using a voltage resistive source, while the output port is terminated with a 50 Ω resistive element to achieve matching. Figure 4 gives two indicative snapshots of the device's surface current distribution during its operation as a mere microstrip or a filter (depending on the EBG frequency range). Finally, Fig. 4 presents the very good agreement between the FVTD (L = 3) results and the measured data from our fabricated prototype.

IV. REFERENCES

[1] F. Yang and Y. Rahmat-Samii, *Electromagnetic Band Gap Structures in Antenna Engineering*, London, UK: Cambridge University Press, 2008.

[2] Y. Li, J. Zhu, Q. Yang, Z. Wei, Y. Guo, and Y. Wang, "Measurement of soft magnetic composite material using an improved 3-D tester with novel sensing coils," *IEEE Trans. Magn.*, vol. 46, no. 6, pp. 1971-1974, 2010.

[3] V. De Santis, M. Feliziani, and F. Maradei, "Safety assessment of UWB radio systems for body area network by the FD^{2}TD method," *IEEE Trans. Magn.*, vol. 46, no. 8, pp. 3245-3248, 2010.

[4] J. Lu, B. Zhu, and D. Thiel, "Full wave solution for Intel CPU in EMC investigations," *IEEE Trans. Magn.*, vol. 46, no. 8, pp. 3405-3408, 2010.

[5] H. De Gersem, R. Schuhmann, S. Feigh, and T. Weiland, "Hierarchical FIT/FE discretization for dielectric subcell interfaces," *IEEE Trans. Magn.*, vol. 44, no. 6, pp. 706-709, 2008.

[6] T. Ohtani, K. Taguchi, T. Kashiwa, Y. Kanai, and J. Cole, "Scattering analysis of large-scale coated cavity using the nonstandard FDTD method," *IEEE Trans. Magn.*, vol. 45, no. 3, pp. 1296-1299, 2009.

[7] L. Bernard, R. Torrado, and L. Pichon, "Efficient implementation of the UPML in the generalized finite-difference time-domain method," *IEEE Trans. Magn.*, vol. 46, no. 8, pp. 3492-3495, 2010.

[8] J. Scott, S. Roxenborg, and A. Parker, "An improved triode model," *in Proc. 6th Regional Convention of the Audio Engineering Society*, pp. 1-9, 1996, Melbourne, Australia.